Optimized Dose of Dendritic Cell-based Vaccination in Experimental Model of Tumor Using Artificial Neural Network

Zahra Mirsanei[1], Sima Habibi[1], Nasim Kheshtchin[1], Reza Mirzaei[1], Samane Arab[2,3], Bahareh Zand[1], Farhad Jadidi-Niaragh[4], Aida Safvati[1], Ehsan Sharif-Paghaleh[1,5], Abazar Arabameri[6], Davud Asemani[6,7], Jamshid Hadjati[1,8]

[1] Department of Immunology, School of Medicine, Tehran University of Medical Sciences, Tehran, Iran
[2] Nervous System Stem Cells Research Center, Semnan University of Medical Sciences, Semnan, Iran
[3] Department of Tissue Engineering and Applied Cell Sciences, School of Medicine, Semnan University of Medical Sciences, Semnan, Iran
[4] Immunology Research Center, Tabriz University of Medical Sciences, Tabriz, Iran
[5] Division of Imaging Sciences and Biomedical Engineering, Faculty of Life Sciences and Medicine, St Thomas' Hospital, King's College London, London, England
[6] Faculty of Electrical Engineering, K.N. Toosi University of Technology, Tehran, Iran
[7] Division of Pediatrics, Liposomal Cancer Therapy, Medical University of South Carolina, Charleston, SC, USA
[8] Cancer Biology Research Center, Cancer Institute of Iran, Tehran University of Medical Sciences, Tehran, Iran

ABSTRACT

Previous studies have demonstrated that maturation of dendritic cells (DCs) by pathogenic components through pathogen-associated molecular patterns (PAMPs) such as Listeria monocytogenes lysate (LML) or CpG DNA can improve cancer vaccination in experimental models. In this study, a mathematical model based on an artificial neural network (ANN) was used to predict several patterns and dosage of matured DC administration for improved vaccination.

The ANN model predicted that repeated co-injection of tumor antigen (TA)-loaded DCs matured with CpG (CpG-DC) and LML (List-DC) results in improved antitumor immune response as well as a reduction of immunosuppression in the tumor microenvironment. In the present study, we evaluated the ANN prediction accuracy about DC-based cancer vaccines pattern in the treatment of Wehi164 fibrosarcoma cancer-bearing mice.

Our results showed that the administration of the DC vaccine according to ANN predicted pattern, leads to a decrease in the rate of tumor growth and size and augments CTL effector function. Furthermore, gene expression analysis confirmed an augmented immune response in the tumor microenvironment.

Experimentations justified the validity of the ANN model forecast in the tumor growth and novel optimal dosage that led to more effective treatment.

Keywords: Cancer; Cancer vaccines; Dendritic cells; Listeria monocytogenes

Corresponding Author: Jamshid Hadjati, PhD;
Department of Immunology, School of Medicine, Tehran University of Medical Sciences, Tehran, Iran. Tel: (+98 21) 6405 3268, E-mail: hajatij@tums.ac.ir

INTRODUCTION

Cancer is currently a major cause of death in the world, and many efforts are underway to find a more effective treatment. Cancer immunotherapy science attempts to employ the power and specificity of the immune system to eliminate tumor cells.[1-4] The ability of dendritic cells (DCs) to uptake and cross-present tumor antigens to cytotoxic T lymphocytes (CTLs) makes DCs a candidate to utilize in cancer vaccination.[5-7] DC-based cancer vaccines are produced based on ex-vivo generated tumor antigen (TA)-loaded DCs that are injected back into the patient.[6] Some investigators have argued that exposing DCs to pathogen-associated molecular patterns (PAMPs) in the antigenic structures of Listeria monocytogenes such as proteins, lipopolysaccharide (LPS) and nucleotide sequences like CpG could fully activate DCs and thus stimulate antitumor immune responses.[8-10] Studies show that exposure to CpG oligonucleotides[11] and Listeria monocytogenes fractions[12] cause further maturation of DCs, increased expression of costimulatory molecules and pro-inflammatory cytokines, more effective antigen presentation and consequently higher proliferation of antigen-specific T cells.

Mathematical modeling provides the means to assess hypotheses, confirm experiments, and simulate the dynamics of complex systems to predict non-conducted clinical trials as well as drug or a vaccine optimal dose selection.[13,14] Based on the experimentally-possible measurements, the interactions of the tumor-immune system cannot be determined in a comprehensively due to the measurement restrictions. However, the proper mathematical models are capable of extracting useful information from experimental data. Modeling tumor-immune system interactions, a black-box methodology which is relying on actual data without any theoretical presumption would be desired.[15] At the same time, a model of nonlinear structure would be indispensable to account for the complicated and varying interactions of the immune-tumor cells.[16] As a suitable candidate, Artificial Neural Networks (ANNs) are nonlinear, black-box models mimicking the structure and function of biological neural networks.[17] ANNs have been broadly used in modeling of complex dynamics such as financial,[18] industrial,[19] and biological systems.[20,21]

In our previous study, the efficacy of different numbers of injections, once, twice and three times injection of DCs matured by adjuvants including Listeria monocytogenes derived lysate (LML) (List-DCs) and CPG nucleotide sequences (CpG-DCs) were accomplished in fibrosarcoma murine models.[22] Then the ANN model was used to optimize the dose/number of DC injections required for an enhancement in tumor immunotherapy.[23] Regarding the complexity of the immune system behavior in response to different types of vaccines and also complicated feedback paths of the immune system, a dynamic recurrent ANN called nonlinear auto-regressive network with exogenous (NARX) model was used to characterize the performance of DC vaccination.[23] Outputs in the dynamic ANN depend on the current and previous input values including initial tumor cell population and vaccination administration profile over the time course.[24] Among the suggested patterns by trained ANN, an exponential administration dose of DCs that confirmed in pilot tests were selected to evaluate as our vaccination pattern.

In this study, DC-based cancer vaccine therapy was performed in fibrosarcoma murine models and the dose/number of administered DCs was selected using the proposed mathematical ANN model. The Predicted exponential pattern of DC vaccination was designed as three consecutive injections of List-DCs combined with the CpG-DCs vaccine, such that the latter decreases and the former increases in dosage. The observed results were then used to assess the accuracy of the mathematical pattern.

MATERIALS AND METHODS

Mathematical Model and Simulation

The data for the mathematical model was obtained from our previous experiments that showed that the effect of multiple injections (once, twice and three times) of TA-loaded CpG-DCs and List-DCs as cancer vaccine in different groups of mice led to different results.[22] The number of injections (once, twice and three times) at a fixed dose (10^6 DCs/injection) along with tumor size of a few consecutive days (except the desired day) were used as ANN inputs and the tumor size in the desired day was used as ANN output. Since the available data volume was not enough to train the ANN, interpolation was used to increase the number of data samples to 21 samples in each group. The procedure of finding the optimal injection pattern by the neural network has two phases: training and prediction phase. In the training phase, the injection

pattern (a sequence, having the value of 10^6 DCs at injection times and 0 elsewhere) of each group was given to PK-PD (pharmacokinetic/pharmacodynamic) model to describe mean blood concentration of DCs. Then, for every desired day, the output of the PK-PD model on the desired day and several days before that, as well as tumor size in several days before the desired day was used as ANN inputs. The error between the tumor size in the desired day and the output of the network was used to train ANN. After training ANN, in the prediction phase, the desired injection pattern can be given to the PK-PD model, the output of which, along with predicted tumor size in several days before the desired day is fed to the trained ANN. The ANN then predicts the tumor size in the desired day at its output. Several injection profiles were simulated by trial and error to find a pattern that minimizes the size of the tumor in the final days. Some patterns were proposed to pretest in experimental models including i) 4 times injection of the vaccine, ii) Exponential profile vaccination.[19] Exponential profile was followed in two patterns: a) Reduction of List-DCs and also increase of CPG-DCs, b) Reduction of CPG-DCs and also increase of List-DCs (not published data). Based on results from our pilots that released contrary to first exponential pattern and more similar to the second one, final optimal pattern to continue the experiments suggests a dose of CPG-DC is reduced in three stages from 1×10^6 to 1×10^5 and dose of List-DC is increased in three stages from 1×10^5 to 1×10^6.

Animals and Cell Lines

This study was conducted according to the Ethics Board approval number 93-02-30-25760 from the Centre research ethics board of Tehran University of medical science. Six- to eight-week-old female BALB/c mice were purchased from the Lab Animal Center, Pasteur Institute of Iran. BALB/c derived fibrosarcoma (WEHI-164) cell line provided by the National Cell Bank of Iran (Pasteur Institute of Iran, Tehran, Iran) was used. Cell lines were maintained in a medium of RPMI 1640 (Sigma, Aldrich, USA), 10% heat-inactivated Fetal bovine serum (Gibco, USA), 100 µg/mL streptomycin and 100 U/mL penicillin (Biosera, UK), and 2mM L-Glutamine (Biosera, UK).

Preparation of Tumor Lysate

Wehi164 cell line was provided and cultured as the above-mentioned. Cell lysates were generated by repeated freeze-thaw cycles (liquid nitrogen and 37°C

water bath). After centrifugation (10 min, 900 g), supernatants were collected and passed through a 0.2-µm pore filter. The supernatant was collected, and the protein concentration was quantified with Thermo Scientific BCA protein assay (Bicinchoninic acid assay) using bovine serum albumin (BSA) as standard.[25]

Oligonucleotides

ODNs (Oligo deoxynucleotide) including CpG ODN 1826 (TCC ATG ACG TTC CTG ACG TT) were obtained from Alpha DNA Company (Montreal, Canada).

Preparation of Listeria Monocytogenes Lysate

Listeria monocytogenes (ATCC 19115) was purchased from the Iranian Research Organization for Science and Technology (IROST). In brief, bacteria were grown in BHI broth media (CONDA, Spain) to mid-logarithmic phase, and a spectrophotometer was used to track changes in the optical density (OD) over time. It is found that the mid-log phase is about 10 hours after inoculation (OD ~0.8). Thus, the bacteria collected after this time point in all experiments. Next step bacteria cultures pelleted and washed in PBS three times. The sonicated suspension was passed through a 0.2 µm filter. Protein concentration was measured using the BCA assay. The LML was stored at-70ºC until use.[12]

Generation of Bone Marrow-derived DCs

Exvivo generation of Bone Marrow-Derived DCs (BMDCs) was performed mainly based on Inaba protocol.[26,27] In the first step, bone marrow hematopoietic stem cells were obtained from the femur and tibia of female BALB/c mice. Then red blood cells were removed by lysing. Following washing with incomplete RPMI (Gibco, USA), cells were plated in RPMI (Gibco, USA) plus 10% heat-inactivated fetal bovine serum (Gibco, USA), 20 ng/mL of recombinant murine GM-CSF (PeproTech, London, UK), and 10 ng/mL of recombinant murine IL-4 (PeproTech, London, UK), 2mM L-glutamine (Biosera, UK), 100 µg/mL streptomycin, and 100 U/mL penicillin (Biosera, UK). On day 3 non-adherent granulocytes and T and B cells were gently removed and fresh media were added. On day 5 loosely adherent proliferating DC aggregates were dislodged and re-plated in fresh cytokines and media supplemented with 100 µg tumor lysate, 10 µg CpG 1826, and 6 µg LML. In all steps,

cells were incubated in a 5% CO2 humidified incubator. Non-adherent mature (m) DCs were harvested on the 7th day of culture. Morphology of mDCs was distinguished by cytospin preparation of the cells using Giemsa stain.

Flow Cytometry and Antibodies

mDCs from the 7th day of culture were stained with FITC-conjugated CD86 (clone: 2F4), MHC-II antibodies (clone: M5/114.15.2) and PE-conjugated CD11c (clone: N418) and CD80 (clone:16-10A1) antibody(BD Pharmingen, USA). In all experiments, appropriate isotype control antibodies with the same Ig class and isotype were used. DC phenotype was determined using FACS analysis system (Beckton Dickinson, Mountain View, CA, USA) and analyzed with FlowJo software (version 7.6.1, USA)

Tumor Inoculation

To generate tumors, BALB/c mice were inoculated subcutaneously (S.C.) in the right flank with 0.2 mL of a single-cell suspension containing 1.5×10^6 WEHI-164 cells. When the tumor was palpable, the shortest and longest surface diameters were measured every 2 days by digital calipers; the tumor area was calculated through multiplying the shortest and longest axes. Mice were sacrificed when tumors became ulcerated, or they reached a size of 400 mm^2. Tissue collection was performed on day 22 (n=5 mice per group). For survival analysis, the five remained mice in each group were under observation for more than 80 days.

Treatment Protocol

Tumor-bearing mice(n=40) were divided into four groups: Group 1) Co-injection of TA-loaded DCs matured by LML and CpG, 2) CpG, 3) LML and 4) control (PBS) group. Each group contained 10 mice (5 *in vitro* assays, 5 in survival course). Treatment started 7 days after tumor inoculation, when tumors were ~25 mm^2 in the area, by injection of around 1.1×10^6 TA-loaded DCs (as a suspension in 0.2 mL of PBS) around the tumor site at 7, 11 and 15 days after tumor implantation. Single therapy groups (CpG-DCs and List-DCs) received a fixed-dose (1.1×10^6 cells per injection) of the DC vaccine and the combinational group received an exponential dose of each vaccine based on the ANN pattern.

Enzyme-linked Immunosorbent Assay (ELISA)

To assess the cytotoxicity activity of lymphocyte,

ELISA test was used for the measurement of the granzyme B (GrB) enzyme as a cytotoxic lymphocyte production.[32]For this end, the 1×10^6 splenocytes (as effector) from all four groups of BALB/c mice bearing WEHI164 tumors were incubated with 80 µg/mL tumor antigen lysate (as target) in complete culture medium at 37°C, 5% CO2 for 78h in a total volume of 1 mL/well in 96 well plates. Supernatants were evaluated by; using the GrB ELISA kit (eBioscience Technology, CA). Each sample was analyzed in duplicate and the mean absorbance for each set of standards and samples was calculated.[29]

Quantitative Real-time Polymerase Chain Reaction for T-bet and FoxP3

The expression of T-bet (as a Th1 marker) and FoxP3 (as a Treg marker) transcription factor were evaluated by quantitative real-time polymerase chain reaction (qRT-PCR). Total RNA was extracted from the spleen specimens; using triazole reagent according to the manufacturer's instructions. Conversion of RNA to complementary DNA (cDNA) was performed by reverse transcriptase and random hexamer provided from the Reverse Transcription reagent kit (Takara, Japan). cDNAs were quantified by real-time PCR using an SYBR Green real-time PCR

master mix (Primer design, UK) on an ABI 7500 detection system (Applied biosystems).[30] Amplification was conducted in a total volume of 20 µL for 40 cycles, 5 s at 95°C and 20 s at 60°C and 20 s at 72°C. CT values for each product were determined after PCR to calculate normalized $2^{-\Delta\Delta CT}$. Values were expressed relative to housekeeping ß-actin. The PCR primers were used as follow:
FoxP3forward,
5′-GCAGGGCAGCTAGGTATCTGTAG-3′
FoxP3revers,
5′-TCGGAGATCCCCTTTGTCTTATC-3′
T-bet forward, 5′-CCATGCCAACTTCTGTCTG-3′
T-bet revers, 5′-CGGGTTGTGTTGGTTGTAGA-3′
β-actin forward,
5′-GGTCATCACTATTGGCAACG-3′
β-actinreverse,5′-ACGGATGTCAACGTCACACT-3′

Statistical Analysis

Statistical analysis was performed; using the SPSS statistical software (SPSS, Chicago, IL, USA).

Comparisons between groups were interpreted using one-way ANOVA with a K-independent t-test. Probability values less than 0.05 were considered

significant. Kaplan–Meier survival curves were analyzed; using logrank tests. GraphPad Prism Software (version 5.0) was used for graphs and statistical analysis. The results have been presented as the mean ± standard error of the mean.

RESULTS

Exponential Profile Vaccination Pattern

The neural network can provide appropriate new patterns after passing two training and prediction phases. In the training phase, the PK-PD model presents the DC vaccine injection pattern for each group as a mean concentration of DCs in blood. Then, for every desired day, the output of the PK-PD model on the desired day and several days before that, as well as tumor size in several days before the desired day was used as ANN inputs. The error between the tumor size in the desired day and the output of the network was

used to train ANN. In the prediction phase, the desired injection pattern can be given to the PK-PD model, the output of which along with predicted tumor size in several days before the desired day is fed to the trained ANN. The ANN then predicts the tumor size in the desired day at its output. Several injection profiles were simulated by trial and error to find a pattern that minimizes the size of the tumor in the final days. The final optimal pattern is shown in Figure1a, which suggests that the dose of CPG-DC be reduced in three-time points, 1×10^6 on day 7 and then 5×10^5 on day 11 and finally 1×10^5 on day 15, and the dose of List-DC increased in three-time points, 1×10^5 on day 7 and then 5×10^5 on day 11 and finally 1×10^6 on day 15. Figure 1 (below) illustrates the simulation results of this vaccine. As expected, with multiple exponential doses of DC vaccine administration (Figure 1b), the Th1 cells are more active, while Treg cells are suppressed (Figure 1c) and the tumor eliminated more quickly (Figure 1d)
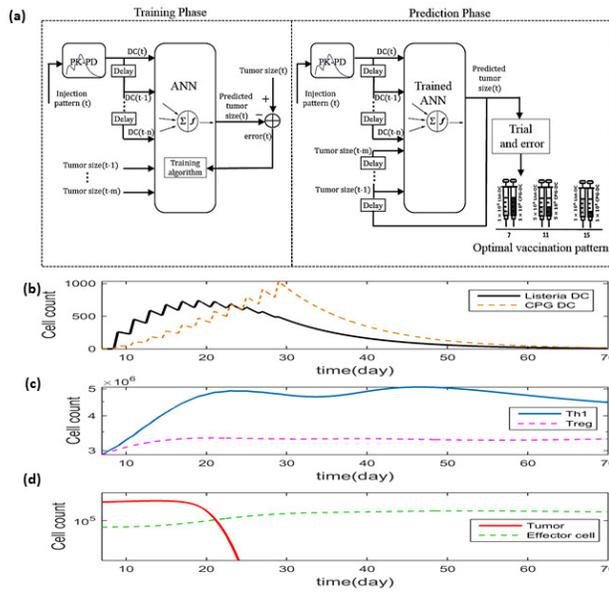

Figure 1. Final nonlinear auto-regressive network with exogenous (NARX) proposed pattern and its prediction of exponential Dendritic cell (DC) vaccination.
(a) After training Artificial neural network (ANN) model using concentration of DCs (obtained by PK-PD model) and tumor size for each group in desired day and several days before that and calculating the errors, in prediction phase, the desired injection pattern can be given to PK-PD model, the output of which along with predicted tumor size in several days before the desired day is fed to the trained ANN. Among the suggested patterns by trained ANN, an exponential pattern of DC vaccine emerged after confirmation by pilot tests. This pattern suggests that the dose of CpG nucleotide sequences loaded dendritic cell (CpG-DC) reduces from 1×10^6 to 1×10^5 and dose of Listeria monocytogenes loaded dendritic cell (List-DC) increases from 1×10^5 to 1×10^6 in three stages. (b) The NARX model predicts that with this DC vaccination pattern, (c) T helper1 (Th1) numbers will be reached its maximum level, while T regulatory (Treg) cells will be reduced to its minimum level and (d) tumor growth will be decreased compared to other predicted patterns (data is not shown).
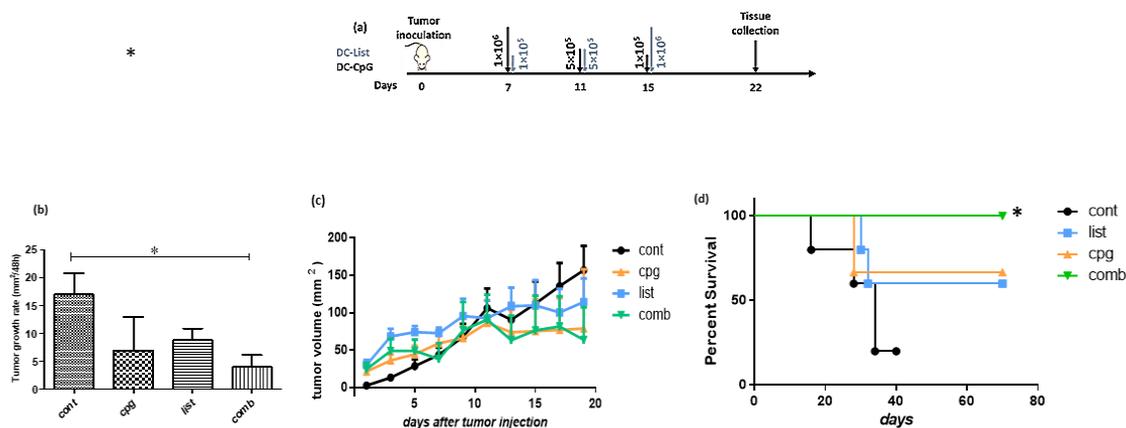
Figure 2. The effect of nonlinear auto-regressive network with exogenous (NARX) vaccination pattern on the survival of tumor-bearing mice and tumor growth. (a) Schematic experimental schedule of dendritic cell-based cancer vaccination. BALB/c mice bearing WEHI 164 tumor were treated by cancer vaccine consisting of List-DCs and CpG-DCs as a combination therapy in an exponential trend of cell doses, List-DCs, CpG-DCs (1.1×10^6 cells, subcutaneously around the tumor site, day 7, 11, 15 of tumor inoculation) and received PBS as control. Each group contained 10 mice. (b) Tumor volume (mean±SEM) reported in mm^2 followed for up to 20 days. (c) The bar chart graph shows the mean tumor growth rate/48 h±SEM. (d) Survival of animals followed up to 80 days in each group (n=5 mice per group) and presented by the respective Kaplan–Meier curves (*p<0.05).

The NARX Pattern of Vaccination Promotes Tumor Regression and Survival of Tumor-bearing Mice

To examine the prediction of NARX pattern about tumor regression, fibrosarcoma tumor-bearing mice were generated and after palpation on day 7, treatment using TA-loaded DCs cancer vaccine was initiated: co-injection of 1×10^6, 5×10^5, 1×10^5 CpG- DCs and 1×10^5, 5×10^5, 1×10^6 of List-DCs was carried out on days 7, 11, and 15 in an opposite trend of doses from each other (Figure 2a). Indeed, this group received the combination therapy in our study along with two other groups received solely List or CpG- DCs on days 7,11 and 15 and a control group (received PBS).

As indicated in Figure 2b and 2c, combination therapy could significantly delay the growth of tumors compared to the control group (Group4) andalso100%mice of group 1 (combination therapy) were alive till the end of the study (Figure 2d). The condition of tumor growth and survival of mice were similar in group 2 (CpG-DCs) and 3 (List-DC).

The NARX Pattern of Vaccination Enhances CTL Activation in Tumor-bearing Mice
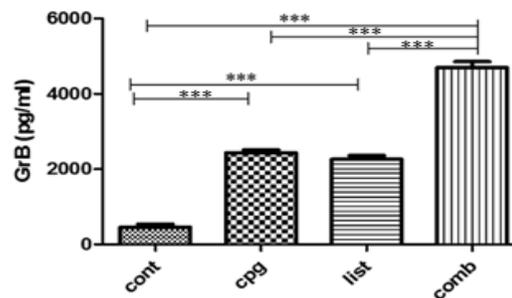
To investigate the mechanism by which NARX

Figure 3. Enhancing the activation of lymphocytes by vaccination based on nonlinear auto-regressive network with exogenous (NARX) pattern.
The Cytotoxic activity of lymphocytes was determined against WEHI-164 tumor antigen as a target. GrB enzyme concentration in the supernatant of splenocytes stimulated by 80 μg/mL of tumor antigen was measured using enzyme-linked immunosorbent assay (ELISA). (*p<0.001; n=5).**

The NARX Pattern of Vaccination Effects Th1 and Treg gene Expression

pattern vaccination restrains tumor growth, the splenocytes cytotoxic activity was evaluated via granzyme B secretion by these cells. Spleen-derived lymphocytes from the mice treated with combination therapy showed significantly higher GrB production compared to the other groups (Figure 3). The level of GrB secretion in single therapy groups was also higher than in the control group.

Previous studies indicated that DC vaccination can induce an inflammatory response.[31-34] To further investigate the mechanism involved in combination therapy, T-bet and FoxP3 gene expression in spleen specimens were evaluated through real-time PCR. This

survey revealed that the combination therapy tends to provoke Th1 immune response significantly (Figure 4a) and also limits the Treg population in a non-significant way in this group (Figure 4b).

Comparison of Empirical Results and ANN Pattern Simulation

As the last step after laboratory experiments, it was necessary to evaluate the accuracy of NARX model predictions about the DC cancer vaccination pattern using the obtained empirical results.

Afterward, the simulation of empirical results was accomplished by a defined NARX model. Figure 5 presents the simulated results and their comparison with the empirical results of injection patterns in all
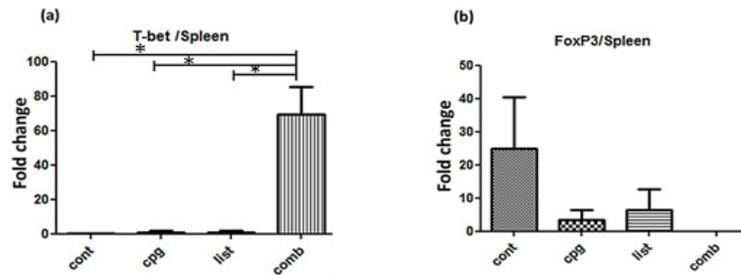

Figure 4. The effect of combination therapy on Th1 and Treg gene expression. WEHI164 tumor-bearing BALB/c mice received DC-based cancer vaccines according to nonlinear auto-regressive network with exogenous (NARX) pattern on days 7, 11 and 15. Spleen specimens were harvested on day 22 after tumor implantation. The expression of T-bet (a) and FoxP3 (b) genes was assessed by real-time RT-PCR. Data are expressed as the mean±SEM; (*$p<0.05$, n=5 mice per group).
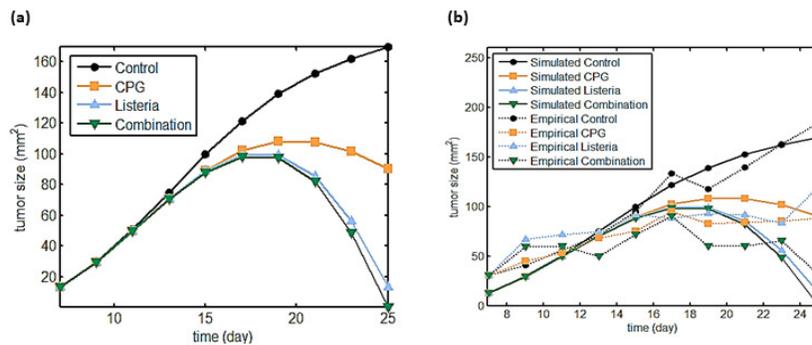

Figure 5. Comparison of tumor volume in experimental and simulated conditions. (a) The nonlinear auto-regressive network with exogenous (NARX) model simulated the trend of tumor size in WEHI164 tumor-bearing BALB/c mice consists of untreated and treated by CpG, List, and both as combination immunotherapy group. (b) Comparison of tumor growth trends obtained from empirical and simulated data for each group.

groups. Concerning fluctuation in primary measurements of tumor size in different groups, a specific real number was added to achieve the same volume as a primary size in all groups, and then the trained NARX model simulated the trend of tumor size for all groups (Figure 5a).

It was expected to attest these simulations by empirical data. To enable better analysis, tumor growth trends obtained from the empirical test (Figure 2c) and model simulation (Figure 5a) are presented for each group in Figure 5b. The comparisons revealed that the empirical findings verified NARX model forecasts for control and combination therapy groups. Based on NARX prediction, these two groups respectively had the worst and the best performance to arrest tumor growth and incite the antitumor immune response, whereas the trend of tumor growth in single therapy groups was not consistent with model simulations. Single therapies act almost similar, and sometimes CpG-DC therapy leads to a better yield in which is not in line with NARX predictions.

DISCUSSION

The crucial role of DCs in driving the immune response makes them an important tool for cancer immunotherapy. Despite the competency of DC-based cancer vaccines to stimulate antitumor immune responses, inhibition of tumor growth and alleviation of patients has failed, and the efforts are still ongoing to strengthen the capacity of DCs to incite specific immune response.[3] Various studies have demonstrated that PAMPs containing bacterial components such as Listeria monocytogenes-derived proteins, LPS and CpG sequences activate DCs through binding to their intracellular or extracellular DCs receptors.[35,39] In a study conducted on the effect of CpG nucleotide sequences on the maturation of dendritic cells, it was found that exposure of DCs to CpG causes further maturation, secretion of IL12 and IL18 cytokines, more effective antigen presentation and higher proliferation of antigen-specific T cells.[11] Another investigation on the effect of different fractions of Listeria monocytogenes on TA-loaded DC maturation and activation of Th1 responses revealed that Listeria monocytogenes could activate DCs and increase the expression of costimulatory molecules and pro-inflammatory cytokines such as IL12.[11] Also, it was

observed that activated DCs are capable of inducing T cells proliferation and secretion of IFN-γ. Moreover, mice receiving List-DCs cancer vaccine demonstrated a minimum tumor growth rate as well as maximum survival in comparison with the control group.[12] Furthermore, combining cancer immunology research with mathematical and computational models in recent years has demonstrated to be beneficial for cancer therapy studies. In a mathematical study of the immune system, Treg cells and TGF-β were counted as suppressive factors and indicated that the use of anti-TGF-β antibody along with the suppression of the Treg population and using DC-based cancer vaccines could stop tumor growth.[44] In another survey dynamics of Treg cells and their plasticity to switch to other CD4+ subtypes was described using ordinary differential equation (ODE) and delay differential equations (DDE).[41] Our study was based on an ANN mathematical model out of which NARX derived from previous empirical results of dendritic cell-based cancer vaccine immunotherapy. The established NARX model predicted a new pattern for DC cancer vaccination in fibrosarcoma murine models asserting that complete tumor regression and maximum prolongation of survival come about if DC cancer vaccination is performed according to NARX pattern. In this study to examine the NARX prediction accuracy fibrosarcoma tumor-bearing mice were injected with TA-loaded CpG-DCs and List-DCs in certain doses and days based on NARX pattern. The process of tumor growth and survival of tumor-bearing mice in treated and untreated groups was monitored during the experiment.

The major finding of the current study is the consistency of the NARX simulations and laboratory findings in the group of mice receiving combination therapy (according to the NARX model) and control (PBS) groups. Indeed, combination protocol resulted in the significant regression of established tumors and increased prolongation of survival, also we observed the worst results in the control group as NARX predicted. Although in single therapy groups (CpG or List-DCs vaccination), the empirical data were different from simulated data. Performances of these two vaccines were similar in terms of cancer immunotherapy or even sometimes the CpG-DC vaccine was more effective. This was in contrary to NARX predictions. After investigating the tumor behavior in the study of groups, we assumed that the

combination vaccine function acted via at least two mechanisms: *i)* Enhancing the effector function of T cells and *ii)* limiting suppressor activity of T cells.

In our previous study, we reported that combination therapy of DC-based cancer vaccination can induce CTL activation and reduce regulatory T cell function.[29] As in another study, it has been shown that combination treatment with TA-loaded-DC and TLR agonists exhibited greater inhibition of tumor growth compared to other groups.[42] These effects were associated with the reduction of suppressor cells, such as regulatory T cells, and the induction of effector cells, such as CD4+ and CD8+ T cells, in the spleen, and with the activation of cytotoxic T lymphocytes.[29,42]

Here, we show that cancer immunotherapy in a combination pattern based on NARX significantly induced CTL activation via GrB secretion. Besides, we observed the decrease of FoxP3 expression and a significant increase of T-bet gene expression in the spleens.

These findings suggested that probably the mechanisms behind the vaccination protocol; using the NARX pattern is to incite the antitumor immune response by Th1 subset and cytotoxic T lymphocytes along with limiting the suppressor T cell population such as Treg cells.

Altogether, it seems that the recruitment of the mathematical and computational science can assist cancer researchers to make predictions and pick out better treatment procedures with lower costs and without exposing researchers or participants to potential risks and open new viewpoints to individual cancer treatments as well. However, it is necessary to note that owing to complexity of tumor environment and lack of sufficient data, achieving a comprehensive mathematical model is not possible and it is desirable to determine several time points for sample sacrificing and tissue collecting during the experiments in order to have more actual data of research to develop a better mathematical model.

REFERENCES

1. Mirzaei HR, Jamali A, Jafarzadeh L, Masoumi E, Alishah K, Fallah Mehrjardi K, et al. Construction and functional characterization of a fully human anti-CD19 chimeric antigen receptor (huCAR)-expressing primary human T cells. J Cell Physiol 2019; 234(6):9207-15.

2. Mirzaei HR, Mirzaei H, Lee SY, Hadjati J, Till BG. Prospects for chimeric antigen receptor (CAR) γδ T cells: a potential game changer for adoptive T cell cancer immunotherapy. Cancer Lett 2016; 380(2):413-23.

3. Namdar A, Mirzaei R, Memarnejadian A, Boghosian R, Samadi M, Mirzaei HR, et al. Prophylactic DNA vaccine targeting Foxp3+ regulatory T cells depletes myeloid-derived suppressor cells and improves anti-melanoma immune responses in a murine model. Cancer Immunol Immunother 2018; 67(3):367-79.

4. Nourizadeh M, Masoumi F, Memarian A, Alimoghaddam K, Moazzeni SM, Yaghmaie M, et al. In vitro induction of potent tumor-specific cytotoxic T lymphocytes using TLR agonist-activated AML-DC. Target Oncol 2014; 9(3):225-37.

5. Palucka K, Banchereau J. Cancer immunotherapy via dendritic cells. Nat Rev Cancer 2012; 12(4):265-77.

6. Timmerman M, John M, Levy M, Ronald. Dendritic cell vaccines for cancer immunotherapy. Ann Rew Med 1999; 50(1):507-29.

7. Rosenberg SA. Progress in human tumour immunology and immunotherapy. Nature 2001; 411(6835):380-4.

8. Muraille E, Giannino R, Guirnalda P, Leiner I, Jung S, Pamer EG, et al. Distinct in vivo dendritic cell activation by live versus killed Listeria monocytogenes. Eur J Immunol 2005; 35(5):1463-71.

9. Krug A, Rothenfusser S, Selinger S, Bock C, Kerkmann M, Battiany J, et al. CpG-A oligonucleotides induce a monocyte-derived dendritic cell-like phenotype that preferentially activates CD8 T cells. The J Immunol 2003; 170(7):3468-77.

10. Khamisabadi M, Arab S, Motamedi M, Khansari N, Moazzeni SM, Gheflati Z, et al. Listeria monocytogenes activated dendritic cell based vaccine for prevention of experimental tumor in mice. Iran J Immunol 2008; 5(1):36-44.

11. Arab S, Motamedi M, Khansari N, Moazzeni SM, et al. Dendritic cell maturation with CpG for tumor immunotherapy. Iran J Immunol 2006; 3(3):99-105.

12. Saei A, Boghozian R, Mirzaei R, Jamali A, Vaziri B, Hadjati J. Listeria monocytogenes protein fraction induces dendritic cells maturation and T helper 1 immune responses. Iran J Allergy Asthma Immunol 2014; 13(1):1-10.

13. Dolgin E. The mathematician versus the malignancy. Nat

Med 2014; 20(5):460-3.

14. Bonin CRB, Fernandes GC, dos Santos RW, Lobosco M. Mathematical modeling based on ordinary differential equations: A promising approach to vaccinology. Hum Vaccin Immunother 2017; 13(2):484-9.

15. Linde J, Schulze S, Henkel SG, Guthke R. Data-and knowledge-based modeling of gene regulatory networks: an update. EXCLI J 2015; 14:346-78.

16. Debnath L. Nonlinear partial differential equations for scientists and engineers: Springer Science & Business Media; 2011.

17. Dreyfus G. Neural networks: methodology and applications: Springer Science & Business Media; 2005.

18. Falat L, Stanikova Z, Durisova M, Holkova B, Potkanova T. Application of neural network models in modelling economic time series with non-constant volatility. Procedia Economics and Finance. 2015;34:600-7.

19. Zamaniyan A, Joda F, Behroozsarand A, Ebrahimi H. Application of artificial neural networks (ANN) for modeling of industrial hydrogen plant. International Journal of Hydrogen Energy. 2013;38(15):6289-97.

20. Khan J, Wei JS, Ringner M, Saal LH, Ladanyi M, Westermann F, et al. Classification and diagnostic prediction of cancers using gene expression profiling and artificial neural networks. Nat Med 2001; 7(6):673-9.

21. Younis A, Ibrahim M, Kabuka M, John N. An artificial immune-activated neural network applied to brain 3D MRI segmentation. Journal of digital imaging. 2008 Oct 1;21(1):69-88..

22. Pourgholaminejad A, Jamali A, Samadi-Foroushani M, Amari A, Mirzaei R, Ansaripour B, et al. Reduced efficacy of multiple doses of CpG-matured dendritic cell tumor vaccine in an experimental model. Cell Immunol 2011; 271(2):360-4.

23. Mehrian M, Asemani D, Arabameri A, Pourgholaminejad A, Hadjati J. Modeling of tumor growth in dendritic cell-based immunotherapy using artificial neural networks. Comput Biol Chem 2014; 48:21-8.

24. Khan J, Wei JS, Ringner M, Saal LH, Ladanyi M, Westermann F, Berthold F, Schwab M, Antonescu CR, Peterson C, Meltzer PS. Classification and diagnostic prediction of cancers using gene expression profiling and artificial neural networks. Nature medicine. 2001 Jun;7(6):673

25. Nestle FO, Alijagic S, Gilliet M, et al. Vaccination of melanoma patients with peptide-or tumorlysate-pulsed dendritic cells. Nat Med 1998;4(3):328-32.

26. Inaba K, Inaba M, Romani N, Aya H, Deguchi M, Ikehara S, et al. Generation of large numbers of dendritic cells from mouse bone marrow cultures supplemented with granulocyte/macrophage colony-stimulating factor. J Exp Med 1992; 176(6):1693-702.

27. Inaba K, Inaba M, Naito M, Steinman R. Dendritic cell progenitors phagocytose particulates, including bacillus Calmette-Guerin organisms, and sensitize mice to mycobacterial antigens in vivo. J Exp Med 1993; 178(2):479-88.

28. Shafer-Weaver K, Sayers T, Strobl S, Derby E, Ulderich T, Baseler M, et al. The Granzyme B ELISPOT assay: an alternative to the 51 Cr-release assay for monitoring cell-mediated cytotoxicity. J Transl Med 2003; 1(1):14.

29. Kheshtchin N, Arab S, Ajami M, Mirzaei R, Ashourpour M, Mousavi N, et al. Inhibition of HIF-1α enhances anti-tumor effects of dendritic cell-based vaccination in a mouse model of breast cancer. Cancer Immunology, Immunotherapy. 2016;65(10):1159-67.

30. Jadidi-Niaragh F, Atyabi F, Rastegari A, Kheshtchin N, Arab S, Hassannia H, et al. CD73 specific siRNA loaded chitosan lactate nanoparticles potentiate the antitumor effect of a dendritic cell vaccine in 4T1 breast cancer bearing mice. J Control Release 2017; 246:46-59.

31. Terhune J, Berk E, Czerniecki BJ. Dendritic Cell-Induced Th1 and Th17 Cell Differentiation for Cancer Therapy. Vaccines (Basel) 2013; 1(4):527-49.

32. Macatonia SE, Hosken NA, Litton M, Vieira P, Hsieh C-S, Culpepper JA, et al. Dendritic cells produce IL-12 and direct the development of Th1 cells from naive CD4+ T cells. J Immunol 1995; 154(10):5071-9.

33. Heufler C, Koch F, Stanzl U, Topar G, Wysocka M, Trinchieri G, et al. Interleukin-12 is produced by dendritic cells and mediates T helper 1 development as well as interferon-γ production by T helper 1 cells. Eur J Immunol 1996; 26(3):659-68.

34. Wesa A, Galy A. Increased production of pro-inflammatory cytokines and enhanced T cell responses after activation of human dendritic cells with IL-1 and CD40 ligand. BMC Immunol 2002; 3(1):14.

35. Zenewicz LA, Shen H. Innate and adaptive immune responses to Listeria monocytogenes: a short overview. Microbes Infect 2007; 9(10):1208-15.

36. Kopp E, Medzhitov R. Recognition of microbial infection by Toll-like receptors. Curr Opin Immunol 2003; 15(4):396-401.

37. Mancuso G, Gambuzza M, Midiri A, Biondo C, Papasergi S, Akira S, et al. Bacterial recognition by TLR7 in the lysosomes of conventional dendritic cells. Nat Immunol 2009; 10(6):587-94.

38. Krug A, Towarowski A, Britsch S, Rothenfusser S,

Hornung V, Bals R, et al. Toll-like receptor expression reveals CpG DNA as a unique microbial stimulus for plasmacytoid dendritic cells which synergizes with CD40 ligand to induce high amounts of IL-12. Eur J Immunol 2001; 31(10):3026-37.

39. Marshall JD, Fearon K, Abbate C, Subramanian S, Yee P, Gregorio J, et al. Identification of a novel CpG DNA class and motif that optimally stimulate B cell and plasmacytoid dendritic cell functions. J Leukoc Biol 2003; 73(6):781-92.

40. Wilson S, Levy D. A mathematical model of the enhancement of tumor vaccine efficacy by immunotherapy. Bull Math Biol. 2012;74(7):1485-500.

41. Wilson S, Levy D. Functional Switching and Stability of Regulatory T Cells. Bull Math Biol 2013; 75(10):1891-911.

42. Vo M-C, Lee H-J, Kim J-S, Hoang M-D, Choi N-R, Rhee JH, et al. Dendritic cell vaccination with a toll-like receptor agonist derived from mycobacteria enhances anti-tumor immunity. Oncotarget. 2015;6(32):33781.